https://doi.org/10.5194/egusphere-2026-4186
Preprint. Discussion started: 24 August 2026

Quantifying Snowmelt-Driven Runoff and Estimating the Regional Water Balance of the Smith River Watershed, Montana, USA

Farhaan Cooverji[1], Eunsang Cho[2], Bailing Li[3,4], Carrie Vuyovich[3], Jennifer M. Jacobs[5], Eunsaem Cho[3,4], Eric A. Sproles[6,7], Samuel E. Tuttle[8]

[1]Department of Geography and Environmental Studies, Texas State University, San Marcos, TX, USA
[2]Ingram School of Engineering, Texas State University, San Marcos, TX, USA
[3]Hydrological Sciences Laboratory, NASA Goddard Space Flight Center, Greenbelt, MD, USA
[4]Earth System Science Interdisciplinary Center, University of Maryland, College Park, MD, USA
[5]Department of Civil and Environmental Engineering, University of New Hampshire, Durham, NH, USA
[6]Department of Earth Sciences, Montana State University, Bozeman, MT, USA
[7]Geospatial Core Facility, Montana State University, Bozeman, MT, USA
[8]Department of Earth and Environmental Sciences, Syracuse University, Syracuse, NY, USA

Correspondence to: Eunsang Cho (eunsang.cho@txstate.edu)

Keywords: Land surface model, Water balance, Snowmelt, Runoff, Evapotranspiration, Sublimation

Abstract. Seasonal snowpacks in snow-dominated watersheds across the western United States play a critical role in sustaining regional water resources by delaying runoff and regulating streamflow. Understanding snowmelt contribution to runoff is essential for quantifying regional water resources. While prior studies have utilized proportional approaches to estimate this contribution, a lack of incorporating the physical processes simulating snowpack evolution yields some uncertainty regarding the fate of deposited snow. This study explored water balance approaches and estimates snowmelt-induced runoff in the Smith River Watershed (SRW) located in Montana for a five-year period between the water years of 2017 and 2021. Annual watershed-averaged water balance analyses were carried out using a Noah Multiparameterization land surface model (LSM) dataset and hybrid observation-model-based approaches. While the hybrid approach provides more accurate estimates for water budget variables, the LSM-based approach was more suitable for the annual water balance analysis due to its ability to close the water budget and simulate relevant hydrological processes. The analysis also revealed that underestimations of evapotranspiration and sublimation in Noah-MP result in an overestimation of runoff. Snow-induced runoff was quantified by separating rain- and snow-generated surface and subsurface runoff using outputs from the Noah-MP dataset and hybrid mass balance approaches. The analysis yielded a value of ~32% (85 mm) of runoff originating from snowmelt during the study period—substantially lower than previous regional estimates (~65%) within the SRW reported in the literature. The study's results highlight the value of utilizing land surface models to accurately quantify snowmelt contributions to runoff in mountain watersheds, and underscore the importance of continued refinement of multi-method approaches for representing watershed hydrology and supporting water resource management in snow-dominated regions of the western United States.

https://doi.org/10.5194/egusphere-2026-4186
Preprint. Discussion started: 24 August 2026

1. Introduction

Regional water supply in the western United States (WUS) relies heavily on winter precipitation stored as the seasonal snowpack and the meltwater it generates during the spring. Delayed runoff from snowmelt during the warmer months plays a critical role in sustaining river flows and aquatic ecosystems, while also meeting the water needs of millions of people and the agricultural, hydropower, and industrial sectors (Bales et al., 2006; Barnett et al., 2005; Fritze et al., 2011; Hammond and Kampf, 2020). The rate of snowmelt directly influences other hydrological processes, such as streamflow and evapotranspiration (ET), with rapid melt events producing proportionally higher runoff and slower melt rates promoting greater soil moisture infiltration and enhanced ET losses (Barnhart et al., 2016). An understanding of snowmelt contributions to streamflow is essential for managing water resources at watershed and regional scales, and for supporting drought assessment and flood control—which are dictated by runoff conditions involving precipitation intensity, soil moisture state, land cover, and human factors (Fassnacht and Records, 2015; Zheng et al., 2018). Additionally, the dual reality of current climate trends and increasing stress of water resources, accurately quantifying snowmelt-driven runoff is a critical step toward more reliable hydrological forecasting and sustainable water management in snow-dominated watersheds.

The Missouri River Basin, located in the north-central region of the United States and draining the largest watershed in North America, is prone to flooding induced by snowmelt and soil saturation, posing risks to life and infrastructure. These snowmelt-driven events have produced some of the basin's most damaging floods, and recent assessments highlight how hydroclimatic variability and climate change may further intensify flood hazard (Reager et al., 2015; NOAA Climate Assessment Report, 2013). As evidenced by the 2019 flood events alone, these flood events affected an estimated 14 million individuals and caused approximately $20 billion in damages (NOAA National Climate Report, 2020; Brunner and Fischer, 2022; Velásquez et al., 2023). In this context, understanding the water balance of the basin, especially in its headwaters is critical since these headwater catchments govern how precipitation is partitioned among snow storage, evapotranspiration, groundwater, and streamflow, thereby controlling the timing and magnitude of flows that propagate through the entire mainstem system.

Regional water balance approaches provide valuable insights into the temporal variations of individual hydrological variables and their effects on streamflow and flood hazard. These methods offer practical, straightforward ways to capture the trends and interactions of hydrological variables, simplifying water cycle dynamics into measurable components that are useful for tracking the fate of both solid and liquid precipitation on the ground (Eagleson, 1978; Farmer et al., 2003; Sivapalan et al., 2011). They form a foundational framework for interpreting a region's hydrology and understanding water storage and fluxes over a given period. In snow-dominated areas like the WUS, water balance methods are particularly effective for characterizing how snowpacks influence the seasonal water distribution. By delaying runoff, reducing winter evaporation, and increasing streamflow during melt seasons, snowpacks fundamentally reshape the hydrological cycle in these areas (Barnhart et al., 2016; Berghuijs et al., 2014). Such analyses are instrumental in assessing how snow-mediated storage and release affect the partitioning of runoff within snow-influenced systems. Land surface models (LSMs) serve as essential tools for regional water balance analyses as

https://doi.org/10.5194/egusphere-2026-4186
Preprint. Discussion started: 24 August 2026

they simulate fluxes and soil water storage changes based on water and energy balances (Quintana-Seguí et al., 2019). LSM outputs provide spatially and temporally continuous estimates of key hydrological variables such as snow accumulation and melt, ET, sublimation, soil moisture, groundwater recharge, and runoff – variables that are often sparse or unavailable from in-situ observational networks (Li et al., 2021; Navari et al., 2024; Lu et al., 2020). The Noah Multiparameterization (Noah-MP) LSM provides numerous parameterization schemes—configurable for simulating hydrological processes based on different physics and parameters (Niu et al., 2011; Li et al., 2022; Mirshafee et al., 2024).

Prior studies have employed a variety of approaches involving precipitation, snow water equivalent (SWE), snowmelt, and runoff variables to estimate snowmelt contributions. A commonly used method calculates the ratio of snowfall to total precipitation (snowfall / total precipitation) to evaluate snowmelt contribution to runoff. Doesken and Judson (1997) estimated snowmelt contributions ranging from 60% to 75% for the WUS; their method has been cited in other studies as well (e.g., Fassnacht et al., 2003; Clow et al., 2012). Barnett et al. (2005) estimated the contribution was between 60% to 90% for the WUS using the ratio of accumulated annual snowfall to total annual runoff (total snowfall / total runoff) and a global macroscale hydrological model. Kapnick & Delworth (2013) applied the same approach, using mean annual snowfall and runoff instead of annual totals, and determined a contribution between 40% and 60%. Serreze et al. (1999) characterized WUS snowpack climatology using SNOTEL data and quantified snowmelt contributions as the ratio of SWE to precipitation (SWE / precipitation), with results ranging from 34% to 80%. Stewart et al. (2004) projected changes in the timing of snowmelt across western North America by estimating snowmelt contributions as the ratio of melt season runoff to total annual runoff, yielding values between 50% to 80%. Mankin et al. (2015) assessed global snow dependence and quantified the amount of human water demand met by snowmelt under historical and future climates using the ratio of snowmelt to total precipitation (snowmelt / total precipitation), reporting values between 40% to 60% for the WUS.

While these methods offer general approximations of snow-derived runoff, they do not consider the full suite of physical processes involved in snowpack evolution—especially the partitioning of rain- and snow-generated runoff and the fate of solid precipitation post-deposition, which are critical for assessing snowpack contributions to subsequent runoff. Li et al. (2017) addressed this limitation by estimating historical and future snowmelt-driven runoff contributions in the WUS using a snowmelt tracking algorithm. They employed the VIC model driven by bias-corrected and downscaled meteorological outputs from ten CMIP5 global climate models. This method, constrained by isotope data, enabled tracking snow- and rainfall-derived runoff across the 1960–2100 period. Importantly, the algorithm accounted for sublimation, evaporation, and infiltration losses of snowmelt, factors that are vital for accurate estimations of snowmelt-induced runoff. Their results indicate that 53% of the total historical runoff originated from snowmelt in the WUS, with projections showing a one-third reduction by 2100 under a high-emission RCP 8.5 scenario. While their algorithm marks a significant advancement by coupling modeled snowpack evolution with the runoff partitioning, the VIC model simulates snowmelt infiltration and subsurface runoff only through the unsaturated soils, without representing groundwater as a distinct component of subsurface water storage. Studies have shown that groundwater plays a crucial role in snow hydrology, especially in regions where delayed subsurface flow contributes

https://doi.org/10.5194/egusphere-2026-4186
Preprint. Discussion started: 24 August 2026

substantially to streamflow (Brooks et al., 2025a). In snow-dominant watersheds, a significant fraction of meltwater does not immediately translate into surface runoff but instead infiltrates into the soil profile and recharges groundwater. This introduces storage-mediated delays that redistribute meltwater over seasonal timescales that sustain baseflow and delay streamflow response (Brooks et al., 2021; Jefferson et al., 2008). Thus, the incorporation of groundwater as a distinct component of the water cycle, along with a simulation of snow contributions to groundwater and subsequent subsurface runoff, can improve the accuracy of snowmelt-induced runoff estimates.

In this study, we employ outputs from the Western Land Data Assimilation System (WLDAS, Erlingis et al., 2021), which is based on Noah-MP forced by the North American Land Data Assimilation System (NLDAS-2, Xia et al., 2012) meteorological fields. WLDAS provides a full suite of hydrological variable outputs at a ~1 km resolution across the WUS. With LSMs like Noah-MP (via WLDAS) supplying a full suite of hydrologic variables, researchers can conduct comprehensive water balance analyses and produce more accurate estimates of snowmelt-driven runoff, because LSMs simulate physical processes that govern snowpack evolution and hydrological fluxes. Through this study we aim to 1) explore the partitioning of the annual water budget defined by precipitation in a snow-dominant watershed in the WUS, and 2) quantify the contribution of snowmelt to runoff within the watershed, through simulating snowmelt infiltration and runoff. We analyze the annual water balance for a five-year period, using a combination of seven datasets including WLDAS, ground observations, and other gridded model outputs and datasets (Sect. 3).

2. Study Area

The study area comprises the Smith River Watershed (SRW) located in the headwaters of the Missouri River basin in Montana, USA. The Smith River is the largest free flowing river in the Upper Missouri, a region that produces a third of the US's wheat, barley, and oats (American Rivers, 2024). The watershed is delineated based on the United States Geological Survey (USGS) gage 06077500 near Eden MT (**Figure 1a**), spanning an area of 4,113 km^2. The watershed's land cover is dominated by temperate or subpolar needleleaf forest, followed by temperate or subpolar shrubland and grassland (North American Land Change Monitoring System, 2020). The third most dominant landcover type is irrigated cropland, covering an area of ~207 km^2. The remainder of the landcover includes wetland, water, urban, and barren land classes. Climatically, the SRW falls within a semi-arid steppe climate zone (Peel et al., 2007), and its elevation ranges from 1070 m to 2880 m (**Figure 1b**). During the five-year analysis period (October 2016 to September 2021), the watershed received an average of 292 mm of solid precipitation and 377 mm of liquid precipitation annually.

https://doi.org/10.5194/egusphere-2026-4186
Preprint. Discussion started: 24 August 2026

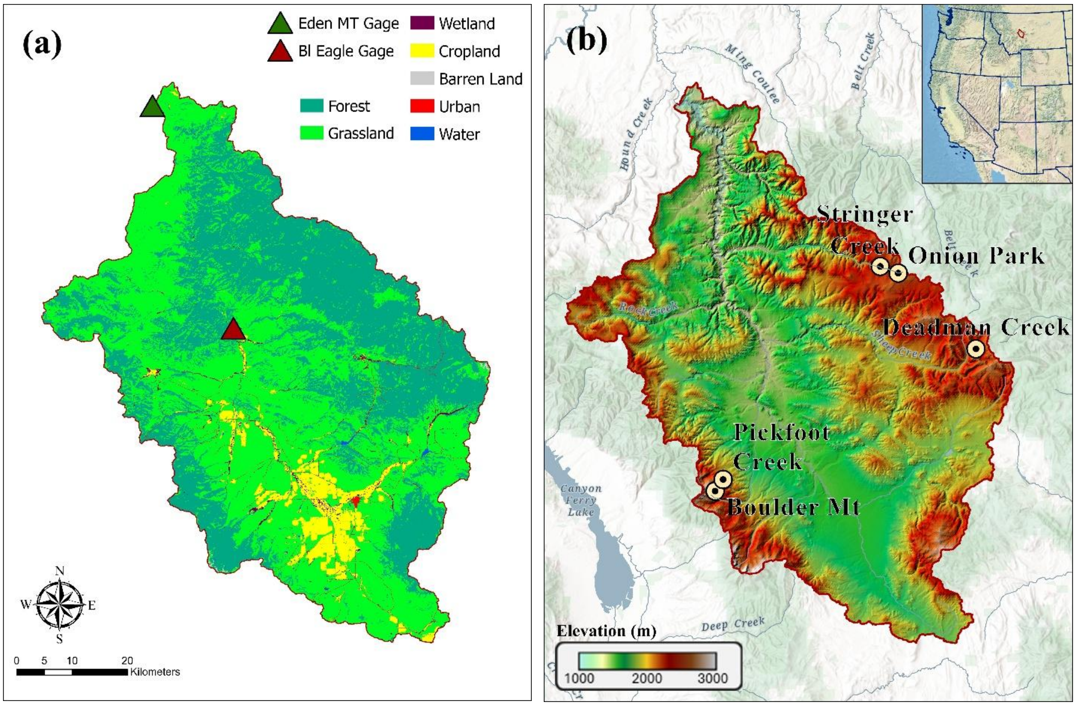

Figure 1: Study area of the Smith River Watershed. (a) landcover types according to the North American Land Change Monitoring System, 2020; and (b) elevational information of the watershed derived from the USGS 3DEP 10m DEM with marked SNOTEL station locations.

3. Data and Models

3.1 WLDAS

WLDAS is an instance of NASA's Land Information System (LIS). It is based on the Noah-MP 3.6 land surface model (Niu et al., 2011) and is driven by the NLDAS-2 meteorological forcing fields, including precipitation and temperature. WLDAS provides daily estimates of water and energy budget components from 1979 to 2023 for the WUS (Erlingis et al., 2021; Erlingis et al., 2024). We used the precipitation, ET, sublimation, groundwater storage, soil moisture, and runoff outputs for LSM-based water balance analysis. In addition, these variables along with WLDAS snowmelt estimates are used to calculate snowmelt-induced runoff within the watershed.

3.2 PRISM

The Parameter-elevation Regressions on Independent Slopes Model (PRISM, PRISM Group) is developed by the PRISM Climate Group at Oregon State University, part of the Northwest Alliance for Computational Science and Engineering (NACSE). PRISM produces daily gridded climate estimates of precipitation and temperature for the conterminous United States at both 4 km and 800 m spatial resolution, with daily data available from 1981 to present. Daily precipitation and temperature data are collected from over 25,000 weather stations including NOAA, USDA,

https://doi.org/10.5194/egusphere-2026-4186
Preprint. Discussion started: 24 August 2026

US Forest Service, and regional networks using the PRISM automated model that interpolates precipitation and temperature fields across areas lacking direct measurements (PRISM Group). PRISM data are widely used in hydrological and climate research due to their spatial continuity, quality-controlled station inputs, and suitability for analyzing climate variability (Daly et al., 2008; Gao et al., 2017, Stern et al., 2022). We used its total precipitation value for our water balance analyses.

3.3 OpenET

OpenET (Melton et al., 2021), a satellite-driven product that provides field-scale actual ET (ETa) and reference ET (ETo) at high spatial resolution across the WUS are used for hybrid water balance analysis. The dataset consists of an ensemble of six peer-reviewed ET models including METRIC, geeSEBAL, DisALEXI, SSEBop, PT-JPL, and SIMS, that are driven primarily by Landsat thermal and optical imagery (30-m resolution) in combination with gridded meteorological inputs (citation). The individual model estimates are combined to produce a single ensemble ET value at daily, monthly, and annual time steps using a monthly arithmetic mean with outliers removed using the Median Absolute Deviation method. Ancillary inputs including crop type maps, soil properties, digital elevation data, and land-cover classifications further inform model parameterization and enhance spatial precision. The OpenET ensemble ET products have been widely adopted for water-budgeting and irrigation management applications due to their multi-model ensemble design, validated accuracy, and open-access implementation (Melton et al., 2021; Volk et al., 2024; Asarian et al., 2025; Montazar et al., 2026).

3.4 SNODAS

The Snow Data Assimilation System (SNODAS) dataset, produced by the National Operational Hydrologic Remote Sensing Center (NOHRSC, 2004), provides daily modeled estimates of SWE, precipitation phase, snowmelt runoff, snow depth, sublimation, and temperature. The dataset is generated using the NOHRSC Snow Model, which incorporates physical, energy, and mass balance-based snowpack modeling driven by downscaled Rapid Update Cycle numerical weather prediction data (Clow et al., 2012). The model assimilates satellite, airborne, and ground-based snow observations using a Newtonian nudging technique to produce estimates of the aforementioned variables from 2003 to present, at ~1 km resolution. SNODAS has been widely used in hydrological applications, including assimilation into rainfall-runoff models for improving runoff simulation (Leach et al., 2018), the optimization of snow monitoring networks by validating hydrologic model calibration (Keum et al., 2018), and integration into runoff models after bias correction to improve representation of basin-scale snow storage (Zahmatkesh et al., 2019). We utilize SNODAS's daily static and blowing sublimation values as water balance variables within our watershed.

3.5 SnowModel

SnowModel is a spatially distributed model that aggregates the MicorMet, EnBal, SnowPack, and SnowTran-3D submodules to simulate snowpack evolution and generate a suite of snow variables for a variety of terrains and elevations (Liston and Elder, 2006). We ran the latest (November 2025) version of SnowModel at a 100 m at a daily timestep for the analysis period, using NLDAS-2 forcing and NALCMS 2020 (30 m) land cover data. The model's

https://doi.org/10.5194/egusphere-2026-4186
Preprint. Discussion started: 24 August 2026

daily sublimation values were used for water balance analyses and to evaluate the estimated sublimation by WLDAS and SNODAS.

3.6 USGS streamflow

We utilized the USGS streamflow observations from gage 06077500 near Eden, MT, as the runoff variable for our water balance calculations. To address missing daily streamflow for the Eden gage during the winter months due to ice bridging (November to March), a gap-filling procedure (Kottegoda and Elgy, 1977) was applied using data from the upstream Eagle gage 06077200 within the same watershed, which closely followed the trend of Eden's streamflow (r = 0.98). Daily streamflow ratios between the two gages were first calculated by dividing Eden flow by Eagle flow for all days with concurrent data availability. Days with missing Eden values were excluded from the ratio calculation. An average of these daily ratios was then computed and used as a scaling factor. For days with missing Eden gage data, streamflow was estimated by multiplying the corresponding Eagle gage value by the calculated average ratio. These adjusted Eden gage streamflow values were then utilized in our water balance calculations by converting the values from cubic feet per day to mm per day.

3.7 LANID irrigation

The LANDSAT-based irrigation dataset (LANID, Martin et al., 2023) provides monthly and annual irrigation values at the Hydrologic Unit Code 12 (HUC 12) scale for the conterminous United States from 2000 to 2020. The dataset combines remotely sensed actual and potential ET (ETa and ETo) from the SSEBop model via OpenET with irrigated area data from the Landsat-based LANID product (citation). The dataset is processed through a modified National Hydrologic Model (NHM) based on the Precipitation-Runoff Modeling System (PRMS) and Coupled Ground-water and Surface-water FLOW (GSFLOW) systems to simulate daily water fluxes and compute consumptive use by HUC 12 region (Martin et al., 2023). Final model outputs include actual evapotranspiration (ETa), irrigation water use, and effective precipitation reported in volumetric units (gallons day^{-1}). These are aggregated to monthly and annual values based on the fraction of irrigated area within each HUC 12 boundary. For integration into our water balance analysis, the model's irrigation consumptive use monthly outputs are converted to watershed-averaged values in mm, and then used to represent irrigation consumptive use.

https://doi.org/10.5194/egusphere-2026-4186
Preprint. Discussion started: 24 August 2026

Table 1. Information on SWE datasets and datasets used in water balance analysis.

Dataset	Spatial Resolution	Temporal Resolution	Relevant Information	Source
WLDAS	1 km	WY 1980 - 2023	Noah-MP forced by NLDAS-2	Goddard Earth Sciences Data and Information Services Center webpage
SNODAS	1 km	WY 2002 - present	NOHRSC sow model; assimilates SWE data from SNOTEL stations	National Snow and Ice Data Center
PRISM	4 km	1981 - present	Data collected from ~25,000 stations including NOAA, USDA, regional networks	PRISM Group at Oregon State University
OpenET	30 m	WY 2000 - present	Satellite-driven ensemble product of six models	Google Earth Engine data catalog
SnowModel*	100 m	WY 2017 – WY 2021	Personal simulation run using NLDAS-2 forcing	*Personal simulation; code provided by Glen Liston
USGS	point	April 1951 – present (intermittent)	Ground observation gage data	National Water and Climate Center (NWCC) webpage
LANID	HUC12 level	2000 - 2020	Processed through NHM using OpenET and Landsat data	ScienceBase.gov

4. Methods

4.1.1 LSM-based water balance

Daily watershed-averaged values of each required WLDAS variable were extracted within the boundary of the SRW for the analysis period of WY 2017–WY 2021. The extracted data were aggregated to yearly totals for each variable to evaluate an annual LSM-based water balance for each of the five water years. An annual water balance equation was utilized as follows:

$$P = ET + Sub + \Delta GW + \Delta SM + Q \qquad (1)$$

where P represents annual precipitation, ET is the annual total evapotranspiration, Sub is annual sublimation, ΔGW is the net change of groundwater storage and ΔSM is the change of soil moisture within the water year, and Q is total runoff. Since ET in the dataset represents total evaporation including sublimation, the Sub variable values were subtracted from each year's ET and presented as a separate variable. ΔGW and ΔSM for each year were calculated by subtracting the corresponding variable value of the first day from the last day of a year.

4.1.2 Hybrid observation-model-based water balances

Hybrid "observation-model-based" annual water balances were also tested since WLDAS sublimation values for the analysis period appeared extremely low (~2.7% per year of the snowpack), and since irrigation water usage is not explicitly represented in the dataset. This alternate water balance approach was aimed at exploring an irrigation-adjusted version of the LSM water balance, as well as a multi-source water balance for the SRW. We utilized hydrologic variables from seven different datasets to display the different water balance variable configurations

https://doi.org/10.5194/egusphere-2026-4186
Preprint. Discussion started: 24 August 2026

available for analyses within the SRW. The hybrid dataset variables include PRISM precipitation (P_h), OpenET evapotranspiration (ET_h), SNODAS sublimation (Sub_h), SnowModel sublimation, adjusted USGS streamflow (Q_h), and LANID irrigation consumptive usage (CU_h).

Daily adjusted USGS streamflow values were converted to runoff (daily discharge divided watershed area), and converted to mm of basin-normalized runoff. Lastly, LANID monthly irrigation reanalysis values available at the HUC 12 scale were extracted as the CU_h variable, accounting for irrigation water use by croplands within the watershed. Monthly CU_h values were only used in water balances incorporating WLDAS ET values, since OpenET accounts for irrigation consumption in its calculations. LANID irrigation values per HUC 12 ID were provided in millions of gallons per day (MGD), representative of the entire month's daily irrigation consumptive use (e.g., 0.24 MGD for October 2016); daily irrigation MGD values were aggregated to monthly values and converted to cubic meters, followed by dividing them by the area of irrigated land for each available year of study period (2016-2020) to yield a mm value for the CU_h variable. The area of land irrigated indicated by LANID records varied from year to year. Monthly irrigation values from the dataset were available only until December 2020; hence, monthly averages for the remaining months of January to September of WY 2021 were taken from the CU_h values of the same months in previous water years of the analysis period to represent WY 2021 (e.g., the value for January 2021 was the average of all January values from the previous years). The calculated monthly CU_h values were then aggregated to yearly totals for the analysis period.

A generic form of the annual water balance equation is provided as the following:

$$P_h = ET_h + Sub_h + \Delta GW + \Delta SM + Q_h + CU_h{}^* \qquad (2)$$

Where * indicates utilizing CU_h values only when WLDAS ET estimates are used. Daily groundwater storage and soil moisture for all hybrid water balances were derived from the WLDAS dataset, while different combinations of datasets for other hydrologic variables were tested to generate hybrid water balances.

4.2 Calculating snowmelt-induced streamflow for the SRW

The contributing fraction of snowmelt to runoff was estimated by accounting for physical processes such as infiltration, subsurface runoff, and partitioning snow- and rain-generated runoff per 1 km pixel within the watershed using WLDAS daily variable outputs. This method was utilized by Li et al (2017) who employed the VIC model, which represents soil moisture as the sole component of subsurface water storage. Using the WLDAS dataset, we incorporated groundwater along with soil moisture as the total subsurface water storage, from which the resultant subsurface runoff is generated (Sect. 4.2.2). The fraction of total snow runoff contribution ($f_{Q,snow}$) at each timestep (t) was derived from the ratio of the sum of snow-generated surface runoff ($SR_{snow,t}$) and subsurface runoff ($SubSR_{snow,t}$) to total runoff in the watershed.

$$f_{Q,snow} = \frac{SR_{snow,t} + SubSR_{snow,t}}{SR_t + SubSR_t} \qquad (3)$$

4.2.1 Snow-generated surface runoff calculation

https://doi.org/10.5194/egusphere-2026-4186
Preprint. Discussion started: 24 August 2026

We first quantified snow-generated surface runoff $SR_{snow,t}$ at each timestep by calculating total infiltration (i_t) and partitioning snow infiltration from rain infiltration (Li et al., 2017). Daily infiltration was quantified using melt (M_t), rain ($Rain_t$), and surface runoff (SR_t) values for the day:

$$i_t = Rain_t + M_t - SR_t \quad (4)$$

Assuming that the fraction of snowmelt infiltration at each timestep is identical to the ratio of melt to the total available water for that day:

$$f_{i,snow,t} = \frac{M_t}{M_t + Rain_t} \quad (5)$$

we calculated snow-generated surface runoff by subtracting snow infiltration from snowmelt for each day (Eq. 6). On days when no snowmelt occurred, the fraction of snowmelt infiltration is set to zero, and the subsequent snowmelt-generated runoff also equals zero:

$$SR_{snow,t} = M_t - (f_{i,snow,t} \times i_t) \quad (6)$$

4.2.2 Snow-generated subsurface runoff calculation

Daily snow-induced subsurface runoff per pixel was derived using a mass balance equation of total groundwater and soil moisture (*WS*) from timestep $t-1$ to t. We assume that the daily fraction of snow-induced subsurface runoff ($f_{SubSR,snow,t}$) is equal to the fraction of total soil moisture and groundwater ($f_{WS,snow,t}$) originating from snow. The same assumption is made for rain-induced runoff. Additionally, an instantaneous input of water from rain and snowmelt to groundwater and the soil moisture layers at the daily timestep is also assumed. The mass balance for groundwater and soil moisture that originated from snow is as follows:

$$WS_{snow,t} = WS_{snow,t-1} + i_{snow,t} - ET_{snow,t} - SubSR_{snow,t} \quad (7)$$

Where $WS_{snow,t-1}$ represents total snow-induced groundwater and soil moisture from the previous day, $i_{snow,t}$ represents infiltrated snowmelt on day, $ET_{snow,t}$ represents evaporated melt water, and $SubSR_{snow,t}$ represents subsurface runoff from snowmelt. Dividing Equation (7) with the total quantity of each variable leads to:

$$f_{WS,snow,t}(GW_t + SM_t) = f_{WS,snow,t-1}(GW_{t-1} + SM_{t-1}) + f_{i,snow,t}(i_t) - f_{WS,snow,t-1}(ET_t) - f_{WS,snow,t-1}(SubSR_t) \quad (8)$$

All values except $f_{WS,snow,t}$ are known, and hence it can be tracked in each timestep. Similarly, the rain-induced fraction of groundwater and soil moisture can be derived from:

$$f_{WS,rain,t}(GW_t + SM_t) = f_{WS,rain,t-1}(GW_{t-1} + SM_{t-1}) + f_{i,rain,t}(i_t) - f_{WS,rain,t-1}(ET_t) - f_{WS,rain,t-1}(SubSR_t) \quad (9)$$

At each timestep, the total water storage below the surface ($WS_{total,t}$) is made up of the sum of snow, rain, and an unknown fraction contributions to groundwater and soil moisture. Thus, $f_{WS,snow,t} + f_{WS,rain,t} + f_{WS,unknown,t} = 1$.

https://doi.org/10.5194/egusphere-2026-4186
Preprint. Discussion started: 24 August 2026

At the first timestep (initial conditions) of the analysis period, the unknown fraction equals 1 while the fractions of snow and rain equal 0, since we do not know the contributions of these two variables to groundwater and soil moisture at that timestep. We use WY 1980 to WY 2016 as a "spin-up" period, during which the mass balance equations (8 and 9) calculate the individual fractions of rain and snow contributions. During this spin-up period, the unknown fraction value approaches 0, while that of rain and snow combined approaches 1. We then calculated snowmelt-induced subsurface runoff at the daily timestep using the following equation:

$$SubSR_{snow,t} = f_{WS,snow,t-1} \times SubSR_t \quad (10)$$

Once daily subsurface runoff values are quantified, we aggregate daily snow-induced surface and subsurface runoff to yearly totals for the analysis period, and utilize Eq. (3) to determine total contribution of snowmelt to runoff per year.

5. Results

5.1 Annual water balance analysis from WLDAS

An annual watershed-averaged water balance was generated using WLDAS modelled outputs, including precipitation, ET, sublimation, fluxes in groundwater and soil moisture, and runoff, to assess the contribution of each variable to the reginal water balance (**Table 2, Figure 2**). Annual total precipitation ranged from 542 mm to 802 mm, with WY 2017 being the driest and WY 2019 being the wettest. Annual ET ranged from 350 mm to 436 mm, and were generally correlated with annual precipitation values. Based on the analysis period from WY2017 to WY2021, approximately 44% of precipitation occurred as snowfall within the SRW. WY 2018 received the highest annual snowfall (359 mm), followed by a gradual decline in subsequent years. ET accounted for the largest water budget component (~400 mm/WY), averaging 61.7% of total precipitation over the analysis period, with its smallest fraction of 54.8% occurring during the second wettest year (WY 2018), and its largest fraction of 68.3% during the second driest year (WY 2021). Runoff followed ET, accounting for 39.6% (~267 mm/WY) of total precipitation on average, peaking up to 346 mm in WY 2018 and dropping to 199 mm during two of the driest years. Groundwater and soil moisture changes were generally small, but exhibited notable interannual variability. WY 2019 saw a substantial soil moisture gain of +61 mm, reflecting enhanced infiltration during the highest-precipitation year, before decreasing to −55 mm in WY 2020. Groundwater storage changes were centered near zero, with the largest positive ΔGW of +17 mm in WY 2018 and a modest depletion to –11 mm in WY 2021. Lastly, we noted that WLDAS sublimation values were notably low each year, ranging from 5 mm to 10 mm and averaging 7.8 mm per year. During the snowiest year, WY 2018, only 2.5% of solid precipitation was lost to sublimation, and values averaged 2.7% of solid precipitation per year over the analysis period.

https://doi.org/10.5194/egusphere-2026-4186
Preprint. Discussion started: 24 August 2026

Table 2: A WLDAS annual water balance displaying total precipitation input (P), including solid and liquid precipitation, along with evapotranspiration (ET), sublimation (Sub), groundwater (GW), soil moisture (SM) and runoff (Q) in mm.

WY	Solid P	Liquid P	Total P	ET	Sub	ΔGW	ΔSM	Q	Difference (in – out)
2017	230	312	542	350	5	2	-14	199	0.3
2018	359	395	754	404	9	17	-22	346	-0.1
2019	313	489	802	436	7	0	61	291	6.0
2020	291	393	684	435	8	4	-55	300	-7.5
2021	267	297	564	375	10	-11	-9	199	-0.7

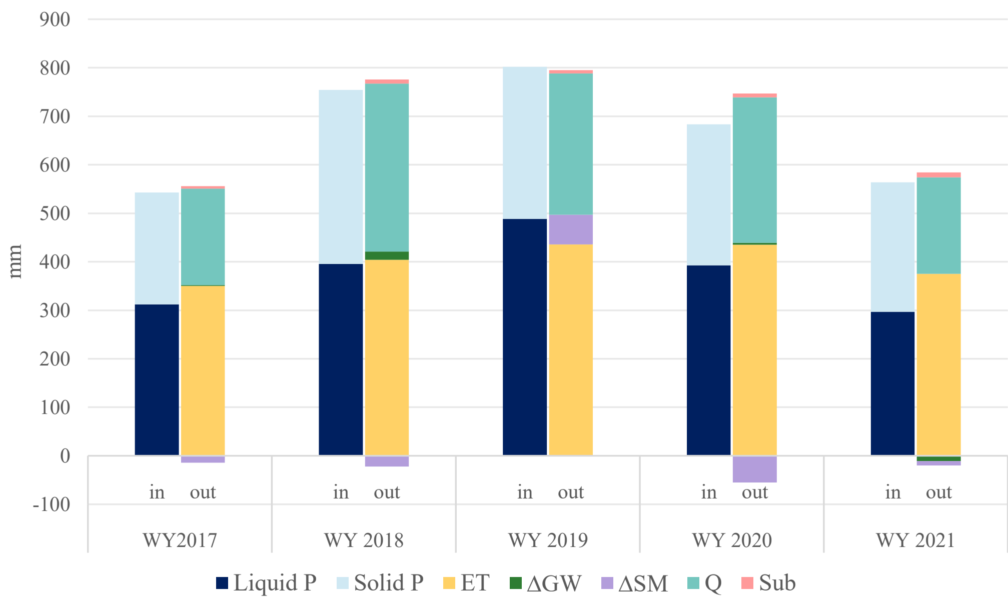

Figure 2: A WLDAS-based annual water balance displaying total water input and output (mm).

5.2 Hybrid annual water balance analysis

To evaluate the reliability of WLDAS variables and derive a more robust water balance estimate for the SRW during the analysis period, we compared WLDAS outputs against a combination of seven independent, well-established datasets—including variables from PRISM, OpenET, SNODAS, SnowModel, USGS, and LANID (**Table 3**)—each recognized for their reliability in representing key hydrological components. To evaluate WLDAS *ET* values, we also utilized LANID *CU* values since irrigation water usage is not simulated in WLDAS; note that we do not use LANID CU estimates when employing OpenET *ET* values, which already incorporate irrigation water consumption.

https://doi.org/10.5194/egusphere-2026-4186
Preprint. Discussion started: 24 August 2026

Table 3: Watershed-averaged water balance variables including precipitation (P), evapotranspiration (ET), sublimation (Sub), runoff (Q), groundwater (GW), soil moisture (SM), and irrigation consumptive usage (CU) provided in mm. LANID-based irrigation values are extracted from irrigated areas within the watershed.

	Total P		ET		Sub			Q		ΔGW	ΔSM	CU
WY	**PRISM**	**WLDAS**	**WLDAS**	**OpenET**	**WLDAS**	**SnowModel**	**SNODAS**	**USGS**	**WLDAS**	**WLDAS**	**WLDAS**	**LANID**
2017	479	542	350	522	5	29	112	44	199	2	-14	15
2018	571	754	404	503	9	33	119	82	346	17	-22	11
2019	555	802	436	494	7	27	84	97	291	0	61	9
2020	463	684	435	539	8	44	126	86	300	4	-55	12
2021	404	564	375	505	10	39	134	36	199	-11	-9	12

https://doi.org/10.5194/egusphere-2026-4186
Preprint. Discussion started: 24 August 2026

Among the various variable combinations examined, we identified two hybrid water balance configurations most appropriate for the SRW: one representing a WLDAS LSM water balance that incorporates LANID-based irrigation estimates, and another that integrates the reliable, independently validated variables across datasets to produce a robust water balance benchmark for the watershed. Specifically, the first hybrid water balance used the *P*, *ET*, *Sub*, *Q*, *ΔGW*, and *ΔSM* values from WLDAS, while also incorporating irrigation usage values from LANID as the *CU* variable (**Table 4, Figure 3**). Since irrigation water usage is not simulated by WLDAS, and since LANID uses ET from croplands as a measurement of how much irrigation water is withdrawn, yearly *CU* values were subtracted from WLDAS *Q* values and represented as an independent variable. This irrigation-adjusted water balance displayed the lowest annual residual storage difference compared to the other water balance combinations tested for the SRW, making it suitable for assessing monthly or yearly regional water resources with the use of LSM variables.

The second hybrid water balance was constructed by integrating variables from multiple independent, well-established datasets: PRISM P, OpenET ET, SnowModel Sub, USGS Q, and ΔGW and ΔSM from WLDAS (**Table 5**, **Figure 4**). Although this configuration yielded a larger residual in water storage, it provides a more reliable estimate of the watershed's water balance by leveraging the individual strengths of each independently validated product. PRISM precipitation values appeared closer to the precipitation values extracted from five SNOTEL stations within the watershed, with a lower average mean absolute difference (1.6 m) compared to that of WLDAS (3.7 m) per WY, and a higher average correlation to each station's total precipitation values ($r = 0.95$) compared to WLDAS ($r = 0.86$). The ensemble OpenET model is widely accepted as being more accurate than individual model estimates in most cases. SnowModel sublimation (*Sub*) values, while higher, were much closer to the values generated by the WLDAS when compared to SNODAS. SnowModel's high resolution (100-m) simulation supported by SnowTran-3D's robust snow physics calculations is considered as a more accurate sublimation variable compared to WLDAS and SNODAS, and is hence more reliable for water balance analyses in the SRW. Lastly, ground-based observation *Q* values available via USGS were used instead of modeled watershed runoff from WLDAS. While USGS *Q* values represented daily streamflow values at the delineation point of the watershed (the Eden gage), after conversion to mm values at the watershed scale these values differed greatly from runoff modeled by WLDAS, and were on average 198 mm lower than the model output values for the analysis period. This can partly be attributed to Noah-MP not incorporating irrigation water usage in its model calculations (Sect. 6.4) and deficiencies in model physics.

https://doi.org/10.5194/egusphere-2026-4186
Preprint. Discussion started: 24 August 2026

381 **Table 4: An irrigation-adjusted hybrid water balance displaying the lowest annual watershed-averaged residual water**
382 **storage difference (mm) from WY 2017-WY 2021. *Q values from WLDAS were adjusted by subtracting LANID**
383 **irrigation values. All variable values are rounded.**

WY	P WLDAS	ET WLDAS	Sub WLDAS	ΔGW WLDAS	ΔSM WLDAS	Q* WLDAS	CU LANID	Difference (in − out)
2017	542	350	5	2	-14	184	15	0.3
2018	754	404	9	17	-22	335	11	-0.1
2019	802	436	7	0	61	282	9	6.0
2020	684	435	8	4	-55	288	12	-7.5
2021	564	375	10	-11	-9	187	12	-0.7

384

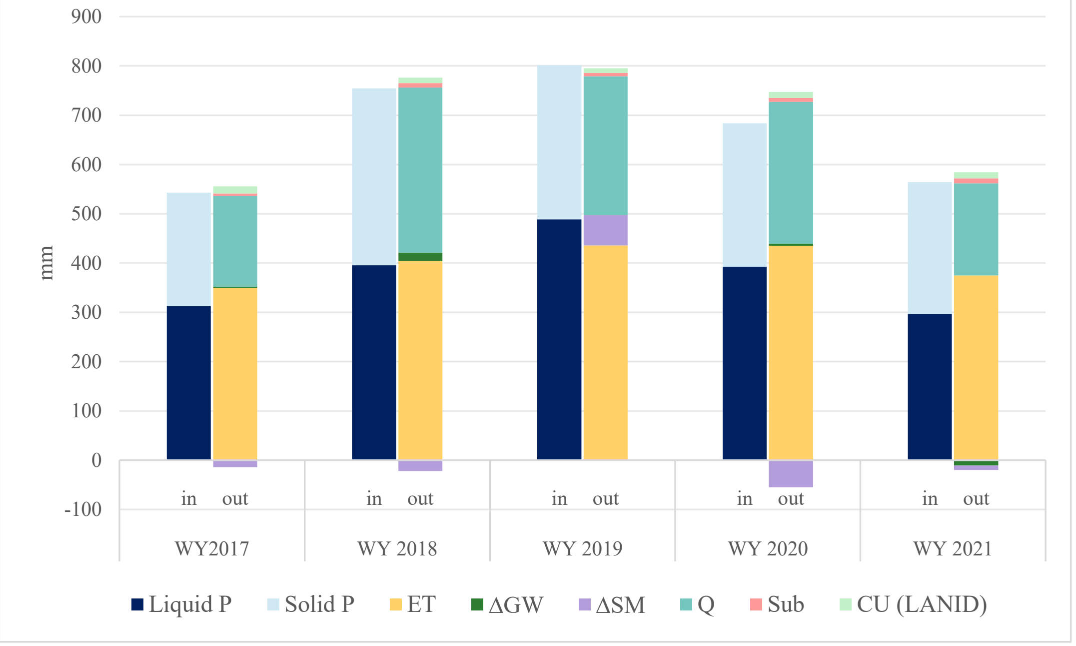

385
386 **Figure 3: An irrigation-adjusted hybrid water balance using land surface model variables from WLDAS with the**
387 **incorporation of LANID irrigation usage values for the SRW (mm).**

https://doi.org/10.5194/egusphere-2026-4186
Preprint. Discussion started: 24 August 2026

Table 5: A watershed-averaged multi-source water balance for the SRW (mm) from WY 2017-WY 2021.

WY	P PRISM	ET OpenET	Sub SnowModel	ΔGW WLDAS	ΔSM WLDAS	Q USGS	Difference (in - out)
2017	479	522	29	2	-14	44	-104
2018	571	503	33	17	-22	82	-42
2019	555	494	27	0	61	97	-124
2020	463	539	44	4	-55	86	-155
2021	404	505	39	-11	-9	36	-156

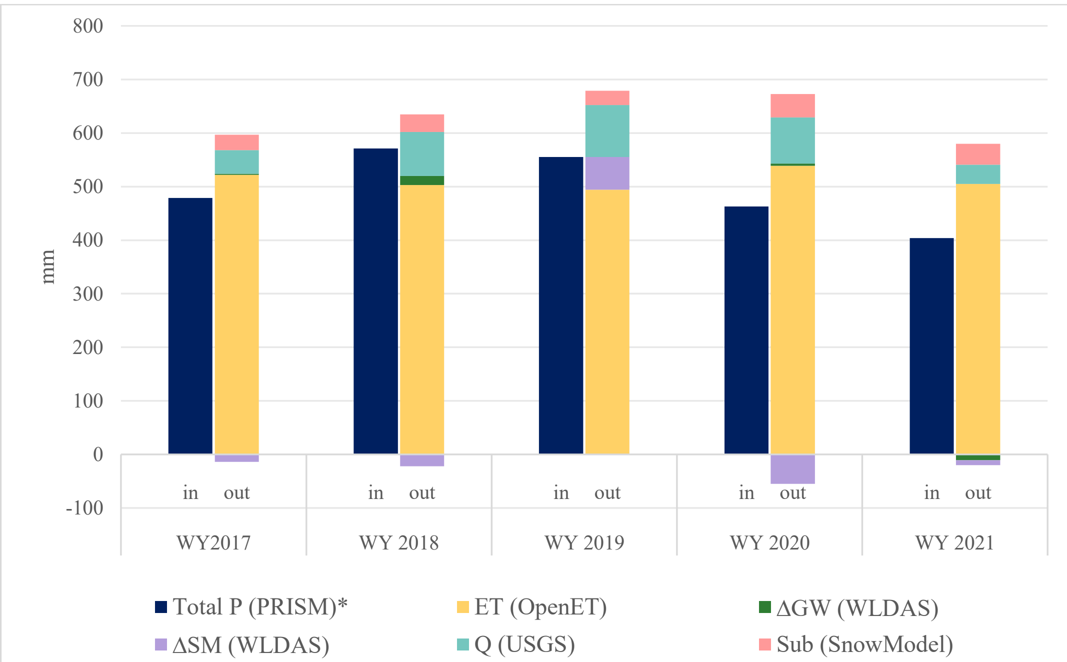

Figure 4: A watershed-averaged multi-source water balance for the Smith River Watershed (mm) from WY 2017-WY 2021. *PRISM data were available only as total precipitation, lacking partitioning in snow and rain precipitation.

We found that ET and sublimation values varied widely across datasets and had a considerable impact on the water balance and annual residual water storage **(Table 6)**. OpenET ET values were consistently higher than WLDAS during the five-year period, ~113 mm higher per WY. Additionally, within the SRW's irrigated area, LANID actual ET values were consistently greater than WLDAS ET estimates (~341 mm higher per WY), which was especially prevalent during the summer months of June through September when irrigation withdrawals made up the highest percentage of ET. Even after incorporating LANID irrigation consumptive use into USGS streamflow to derive an adjusted annual runoff total, the total runoff remained notably lower than the runoff simulated by WLDAS.

https://doi.org/10.5194/egusphere-2026-4186
Preprint. Discussion started: 24 August 2026

Sublimation values from the datasets of WLDAS, SnowModel, and SNODAS also displayed a wide range of values within the SRW. WLDAS sublimation was by far the lowest in terms of raw sublimation values and percent of snowpack sublimated, while SNODAS was the highest for both. Based on each dataset's annual accumulated snowfall, ~3% of snow sublimated annually according to WLDAS, ~17% by SnowModel, and ~43% by SNODAS for the analysis period (**Table 6**).

Table 6: WLDAS, SnowModel, and SNODAS watershed-averaged snow sublimation (mm) from WY 2017-WY 2021.

	Snowfall			Sublimation			% Sublimated		
WY	**WLDAS**	**SnowModel**	**SNODAS**	**WLDAS**	**SnowModel**	**SNODAS**	**WLDAS**	**SnowModel**	**SNODAS**
2017	230	174	320	5	29	112	**2%**	**17%**	**35%**
2018	359	262	472	9	33	119	**3%**	**13%**	**25%**
2019	313	231	275	7	27	84	**2%**	**12%**	**31%**
2020	291	186	235	8	44	126	**3%**	**24%**	**54%**
2021	267	178	193	10	39	134	**4%**	**22%**	**69%**

5.3 Snowmelt-induced runoff within the SRW

Snowmelt-induced surface runoff ($SR_{snow,t}$) was first quantified by separating snow infiltration from rain infiltration, followed by subtracting snow infiltration at each timestep from snowmelt at each timestep to yield snowmelt-induced surface runoff (Eq. 6). We estimated that ~32 mm of yearly surface runoff originated from snowmelt, accounting for 45% of total surface runoff in the watershed for the analysis period. Snowmelt-induced subsurface runoff ($SubSR_{snow,t}$) was calculated next, using a groundwater and soil moisture mass balance equation (Eq. 8), estimating a value of ~53 ± 7 mm for the analysis period, with snowmelt accounting for ~27 ± 8% of total subsurface runoff. The subsurface runoff calculations utilized WYs 1980 to 2016 as "spin-up" years to reduce the unknown fraction of subsurface water origin to 0. However, after the spin-up period the average unknown fraction value ($f_{WS,unknown,t}$) reached 0.17 at the start of the analysis period and 0.15 at the end, corresponding to a watershed-averaged uncertainty in subsurface water origin of 17% at the start of WY 2017, with a continuous and gradual decline to 15% at the end of WY 2021 (further discussed in Sect. 6.3). **Figure 5** displays the average uncertainty per pixel within the watershed during the analysis period, with low-lying areas displaying the largest uncertainty in subsurface runoff origin and high elevation regions displaying the lowest uncertainty.

https://doi.org/10.5194/egusphere-2026-4186
Preprint. Discussion started: 24 August 2026

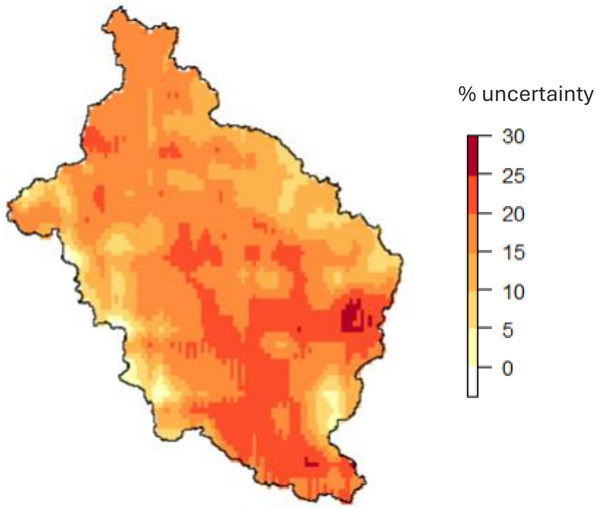

Figure 5: Average uncertainty in the origin of subsurface water storage (groundwater and soil moisture) in terms of contribution from rain or snow between WYs 2017 and 2021.

There was a noticeable lag in surface and subsurface runoff responses to snowmelt, with subsurface runoff lagging approximately one month behind snowmelt input (**Figure 6**). Surface runoff responses typically peaked from March through May, with negligible contributions during the remaining months. Subsurface runoff typically peaked from March through August, and exhibited low but continuous contributions during the remaining months. As for the total contribution of snowmelt to total runoff within the SRW (Eq. 3), the analysis yielded a value of ~85 mm per year, or ~32% of total runoff for the analysis period of WY 2017–WY 2021. Snowmelt contribution to runoff was highest in WY 2018, followed by a gradual decline in the subsequent years, coinciding with the trend of solid precipitation. WY 2017 exhibited the lowest values for snow-induced surface and subsurface runoff. Corresponding with peak SWE magnitude patterns, the high elevation regions of the watershed dominated surface and subsurface runoff during the analysis period (**Figure 7b**). The southwest and southeast regions of the watershed displayed the highest amount of snowmelt runoff, ranging from 500 to 700 mm. Snow-generated surface runoff was lowest for the low-lying and mid-elevation regions, ranging from less than 50 mm to about 100 mm; the high-elevation regions produced roughly 150 mm to 200 mm. Snow-generated subsurface runoff also exhibited elevation-based patterns, with low-lying and mid-elevation regions showcasing the lowest runoff, ranging from below 50 to 100 mm, and higher elevations contributing to 200 to 350 mm on average. Lastly, snow-induced surface runoff provided the highest contribution to total snow runoff in low-elevation regions (**Figure 7c**). In contrast, snow-induced subsurface runoff contributed the highest to total snow runoff in the high-elevation areas, with mountainous regions in the northeast and the southwest of the watershed generating ~70-80% of subsurface runoff (**Figure 7f**). This difference can be attributed to average subsurface water storage being greater in higher elevation regions in the watershed, producing proportionally higher subsurface runoff in these elevations, and due to forested landcover reducing runoff efficiency and promoting greater infiltration in these elevations compared to low-lying areas.

https://doi.org/10.5194/egusphere-2026-4186
Preprint. Discussion started: 24 August 2026

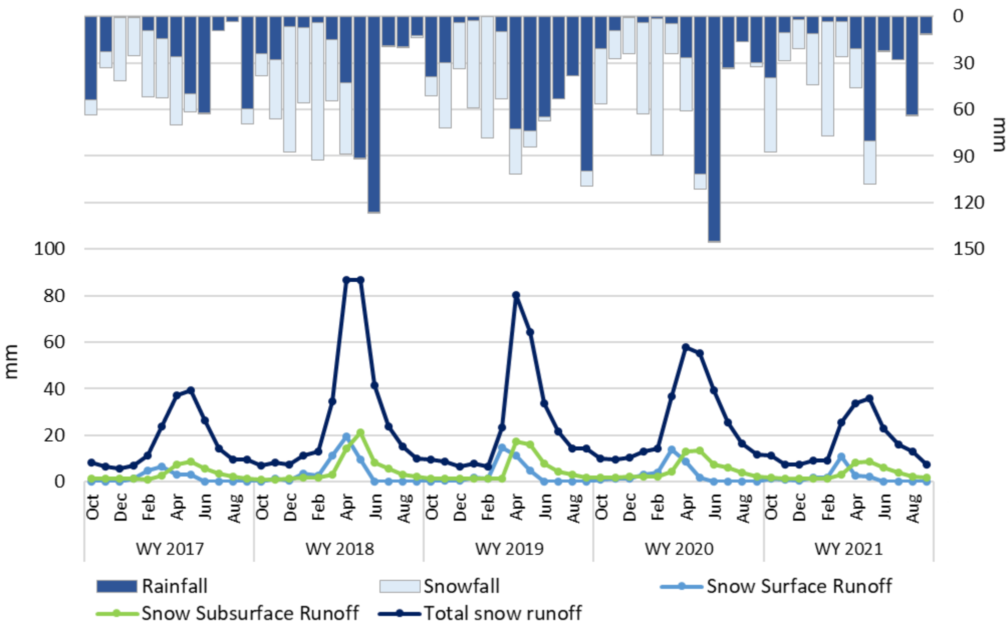

Figure 6: Monthly averaged rainfall and snowfall compared to total monthly runoff and snow-generated surface and subsurface runoff (mm).

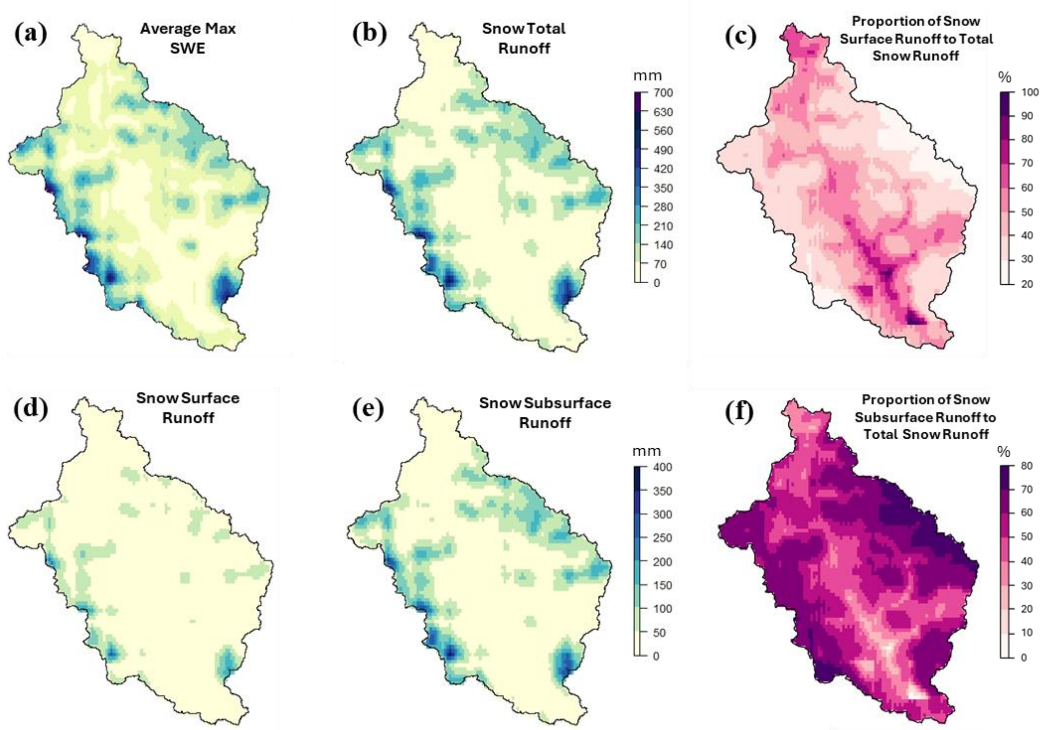

https://doi.org/10.5194/egusphere-2026-4186
Preprint. Discussion started: 24 August 2026

Figure 7: Maps displaying (a) Average maximum SWE, and snow-induced (b) total runoff, (d) surface runoff, and (e) subsurface runoff for WY 2017-WY 2021 (mm). The proportion of snow-induced (c) surface runoff and (f) subsurface runoff to total snow-induced runoff are depicted are percentages per pixel.

6. Discussion

6.1 Water balance analyses employed in prior studies

Prior studies have utilized varied methods to quantify regional water balances for varying purposes, including a focus on estimating the value of specific variables, water storage changes, and impacts on runoff over varying time periods. The sensitivity of ET and runoff efficiency—defined as the ratio of basin outflow to precipitation input—to precipitation variability has been a central focus of certain regional water balance studies, yet the degree of that sensitivity appears to differ markedly across climatic and physiographic settings. Hedrick et al. (2020) documented this dynamic in the Tuolumne River basin from 2015 to 2017, where ET remained relatively stable (~150–300 mm) across a wide precipitation range (547–2,211 mm), while runoff efficiency varied dramatically (53 ± 5% to 82 ± 8%), reflecting the dominant role of snowmelt and precipitation phase in controlling basin outflow. Our results from the SRW suggest a fundamentally different hydrological regime. Both ET products showed comparably low interannual variability (350–436 mm from WLDAS; 494–539 mm from OpenET), consistent with the buffered ET response observed by Hedrick et al (2020). However, unlike the Tuolumne basin, where a wide precipitation range drove large swings in runoff efficiency, precipitation within the SRW fluctuated considerably less (542–802 mm), and runoff efficiency remained relatively consistent and stable across years (35–46%). This contrast likely reflects the comparatively limited snow component in the SRW relative to the Tuolumne basin, where a substantial snow fraction amplifies the phase-driven variability in basin outflow. Together, these differences suggest that while ET may behave as a relatively buffered component across diverse watershed settings, the sensitivity of runoff efficiency is strongly conditioned by the precipitation regime and the degree to which snowmelt contributes to basin outflow.

Denver et al. (2025) employed an error-based annual water budgeting approach from WYs 2015 to 2023 for seven experimental watersheds in the Upper Lake Mary watershed in Arizona. With precipitation as the yearly input, the authors estimated the largest outgoing flux to be through ET (72%), followed by surface runoff (19%) and groundwater recharge (9%). For our study, WLDAS ET dominated outgoing flux (~62%) and surface runoff comprised a significantly smaller portion of flux (10%), while the inclusion of subsurface runoff represented a flux of 30%. Similar to the study in Upper Lake Mary, groundwater recharge in the SRW did not occur every year during the analysis period and only accounted for ~1% of outgoing flux. Their annual water budget errors varied per watershed, ranging from 8% to 62%, attributed to errors in precipitation data, the McNaughton and Black (M-B) model used for simulating ET, and streamflow observations. While the WLDAS water balance for our study yielded minimal residual storage differences per WY (<1% or 3.2 mm) which is expected as WLDAS output are constrained by water and energy balances, the hybrid water balance yielded consistent errors averaging about ~25% for the analysis period. Lastly, Dozier and Melack (1989) utilized a similar catchment-scale water balance approach for a case study of the Emerald Lake watershed in the Sierra Nevada (~1.2 km^2) from 1986 to 1987, exclusively using field measurements of SWE,

https://doi.org/10.5194/egusphere-2026-4186
Preprint. Discussion started: 24 August 2026

gaged precipitation, ET and sublimation (using Penman potential ET calculations and snow-surface energy-balance calculations), and streamflow discharge records. A simple mass balance equation of precipitation input, losses to the atmosphere, and total streamflow was utilized, yielding an error of 40 mm for the analysis period.

While the employment and resultant inferences of these water balance approaches were unique to each study, they display the versatility and applicability of water balances for hydrological studies. This study within the SRW showed how different variables contribute to the water cycle, while showcasing the importance of using datasets produced by numerical simulation, which provides a full suite of hydrologic variable estimates to support mass balance calculations with minimal residual storage. While relying on in situ data and utilizing datasets that most accurately represent each variable in the water cycle would be preferred for quantifying regional water resources, it is expected that assembling a hybrid combination of these variables would degrade the water balance closure. This is because each variable, despite being independently reliable, still carries its own inherent uncertainties and biases that propagate into the overall water balance. While LSM-based water balances display minimal annual storage differences, they can also lack accuracy in certain variables, such as the underestimation of ET and sublimation and the overestimation of runoff by Noah-MP. Improved model parameters and physics have the potential to maintain low annual residual storage differences and improve the accuracy of hydrologic variable estimates (Sect. 6.4).

6.2 Sublimation estimates from WLDAS, SNODAS, and SnowModel

Yearly sublimation values estimated by WLDAS, SnowModel, and SNODAS differed greatly during the analysis period, representing 3%, 17%, and 43% of snowpack sublimated from incoming snowfall, respectively. Relative to SnowModel's robust snowpack sublimation processes, WLDAS (via Noah-MP) utilizes a simpler quantification approach for its calculations: Noah-MP computes sublimation from ground snow and canopy-intercepted snow as a latent-heat flux using Penman/bulk-aerodynamic formulations, with fluxes constrained by the available snow mass in a prognostic multilayer snowpack and canopy-interception scheme (He et al., 2023). This 1-d energy-balance-based sublimation approach is expected to yield low values since snow redistribution is not accounted for. SNODAS sublimation, on the other hand, is estimated as a diagnostic output from the multilayer SNTHERM.89 scheme, based on snow energy- and mass-balance calculations and archived alongside other diagnostic fluxes. SNODAS sublimation is tightly coupled with data assimilation (DA) and empirical adjustment procedures, and does not explicitly simulate lateral redistribution of blowing snow between exposed and sheltered terrain (National Operational Hydrologic Remote Sensing Center, 2004; Jordan, 1991). As SNODAS generates its modeled SWE estimates and assimilates SWE data from respective station networks, sublimation can appear overestimated as a diagnostic result when the model nudges SWE closer to the reference data. SnowModel, through MicroMet, EnBal, SnowPack, and SnowTran-3D, uses distributed surface energy-balance calculations together with explicit wind-driven redistribution and erosion to quantify both static and blowing-snow sublimation across complex terrain (Liston and Elder, 2006). SnowModel partitions losses into surface, canopy-intercepted, and blowing-snow components, driven by locally varying wind fields, topography, and vegetation structure, which yields a more physically explicit representation of sublimation pathways in complex terrain. While the watershed lacks reference data to evaluate yearly sublimation ranges, SnowModel's process-driven sublimation outputs are preferred for incorporation into multi-source water

https://doi.org/10.5194/egusphere-2026-4186
Preprint. Discussion started: 24 August 2026

balances, especially at the watershed scale, because of its representation of physical processes involved. Furthermore, there is a need for studies comparing the physics and outputs of these models along with other available gridded datasets providing sublimation values for the U.S. Quantifying model differences based on terrain, elevation, landcover, and validation against eddy covariance, such as those provided by AmeriFlux stations, could provide valuable insight into each model's sublimation estimates based on the employed model physics.

6.3 Snowmelt-induced runoff uncertainty

Snowmelt-generated runoff was calculated for WY 2017–WY 2021, using WY1980–WY 2016 as spin-up years to reduce the unknown fraction of *WS*. The accuracy of partitioning rain and snowmelt contribution to *WS* depends on the value of the unknown *WS* fraction, which nears 0 with each timestep during the spin-off period. This uncertainty can likely be attributed to the lagged response of groundwater to other near surface processes such as precipitation and soil moisture Monthly computations for this mass balance were also tested, but had insufficient timesteps to reduce the fraction of unknown *WS* sufficiently. Uncertainty in contribution source was lowest for higher elevation regions, and vice versa for lower elevations (**Figure 5**). There was no discernable correlation between the spatial patterns of combined subsurface water storage and uncertainty in subsurface runoff origin across the watershed. The largest uncertainty (~20-27%) was prevalent in the flat, low-lying grassland and cropland regions, and the highest uncertainty (>25%) surrounded wetlands and urban areas.

Using a coarser VIC model, Li et al. (2017) indicated that the HUC 08 unit, within which the SRW is found, is estimated to historically (years 1950 - 2005) generate close to 65% of runoff from snowmelt, more than doubled our estimates. While our analysis only tested five water years, our estimations (32%) deviate from those of Li et al. (2017). This discrepancy could be attributed to Noah-MP simulating groundwater storage changes, while VIC does not. Additionally, the SRW in this study includes about two-thirds of the HUC 08 region, with the remaining third of the HUC 08 region being snow-dominant. Our study found higher runoff generation in the snow-dominated regions as compared to regions having shallower snowpacks. Further analyses are needed to determine if long-term changes in the area's snow regimes have occurred that would account for this discrepancy in snowmelt-induced runoff estimates.

6.4 Limitations and future direction

While LSMs such as Noah-MP can provide datasets with high spatial and temporal resolutions that are particularly useful in regions with limited ground-based observations, uncertainties remain in the estimation of certain variables due to deficiencies in model physics and uncertainties in meteorological forcing fields (Wu et al., 2021; Cho et al., 2022; Sthapit et al., 2022). Noah-MP appears to underestimate total ET in the SRW and does not explicitly account for irrigation water withdrawals, which contribute to its higher runoff estimates compared to USGS gage observations. Other studies employing the model have reported an overestimation of runoff compared to ground observation data as well, particularly in western and arid U.S. basins, due to excessive runoff generation, underestimated ET, and biased precipitation forcing, as reported in the Rio Grande and Lower Colorado basins, across WUS watersheds, and in national-scale model evaluations (Ma et al., 2017; Su et al., 2024; Wu et al., 2021; Zheng et al., 2023). Uncertainties in NLDAS-2 forcing data also contribute to measurable biases and uncertainties in the

https://doi.org/10.5194/egusphere-2026-4186
Preprint. Discussion started: 24 August 2026

LSM's variable estimations, particularly precipitation, SWE, surface energy fluxes, runoff, and soil moisture estimates (Cho et al., 2022; Sthapit et al., 2022; Nearing et al., 2016; Ferguson and Mocko, 2017). While data from PRISM, OpenET, and USGS provide more realistic estimates for their respective variables, annual water input and output balancing proves difficult when using a combination of these datasets, as depicted in Results section (Sect. 5.2). Therefore, employing LSM-generated variables remains a more suitable approach for conducting water balance analyses.

For future analysis using Noah-MP, forcing improvement and DA approaches would translate to better estimations of hydrologic variables, and therefore a further improvement in the accuracy of estimating snowmelt contribution to runoff and the quantification of available water resources. Advancements to the LSM (Noah-MP version 5.0) demonstrate improved performance over previous versions through updated snow parameters and model physics (He et al., 2025). Lastly, NLDAS-3 (1 km) represents an improvement over NLDAS-2 (12.5 km), incorporating gauge observations, satellite retrievals, modeled fields, and machine-learning-based bias correction (Mocko et al., 2024). As daily Noah-MP outputs from NLDAS-3 become available, similar hydrological analyses would benefit from utilizing this high-resolution, enhanced forcing framework, and advanced hydrological processing and parameterizations.

7. Conclusions

This study quantified annual water balances and snowmelt contributions to runoff in the Smith River Watershed (WY 2017–2021), revealing important insights into both the hydrological behavior of the watershed and the limitations of current modeling approaches. WLDAS-based analyses showed that annual ET and sublimation were consistently underestimated relative to independent datasets, driven by simplified snow physics and the absence of irrigation modeling—limitations that motivated the development of a hybrid observation-model water balance using PRISM, OpenET, SNODAS, and USGS streamflow. Despite offering more physically representative estimates of individual components, the hybrid balance revealed persistent closure challenges, underscoring a broader difficulty in using independently sourced datasets with their own systematic biases. Snowmelt-induced surface and subsurface runoff were independently calculated for the analysis period and contributed approximately 32% of total runoff, affirming the hydrological significance of seasonal snow in this watershed. These findings highlight that accurately characterizing regional water balances in snow-influenced systems requires not only careful dataset selection, but also improved physical process representation. Adoption of NLDAS-3 forcing data and updated Noah-MP parameterizations would be a meaningful step toward reducing residual storage discrepancies and strengthening watershed-scale water resource assessments across the WUS.

https://doi.org/10.5194/egusphere-2026-4186
Preprint. Discussion started: 24 August 2026

Code availability

The codes will be made publicly available through a GitHub repository upon publication.

Data availability

All data employed for this study are publicly available. Files for the Noah-MP WLDAS dataset (Daily 0.01 degree x 0.01 degree Version D1.0) were accessed through the NASA Goddard Earth Sciences Data and Information Services Center portal (https://disc.gsfc.nasa.gov/). Files from individual datasets are accessible via the respective sources: SNODAS (https://nsidc.org/data/g02158/versions/1), PRISM (https://prism.oregonstate.edu/), OpenET (GEE data catalog: OpenET Ensemble Monthly Evapotranspiration v2.1), SnowModel (requested from Glen Liston), USGS (https://nwcc-apps.sc.egov.usda.gov/), LANID (https://www.sciencebase.gov/).

Author contribution

FC led the investigation, conceptualized the study, conducted the formal analysis, and wrote the original draft of the manuscript. EC1 (Eunsang Cho) conceptualized the study, acquired the funding and resources, supervised the project, and oversaw the investigation. BL, CV, JMJ, and EC2 (Eunsaem Cho) contributed to the investigation, co-supervised the project, and provided technical and scientific input throughout the study. EAS and SET also co-supervised the project and provided technical and scientific input throughout the study. All authors reviewed and edited the manuscript and approved the final version.

Competing interests

The authors declare that they have no conflict of interest.

Acknowledgements

This work was supported by the NASA Subseasonal-to-Seasonal Hydrometeorological Prediction grant number 80NSSC24K1278, and the Bureau of Reclamation Snow Water Supply Forecasting Program FY 2023 grant number R24AC00021-00. We appreciate the guidance provided by Mike Durand regarding the snowmelt-induced runoff calculations, as well as the support provided by Glen Liston and his team with running SnowModel.

References

American Rivers. (2024). Missouri River. American Rivers. https://www.americanrivers.org/river/missouri-river/

Asarian, J. E., Stanford, B., Murphy, N. P., & Pollock, M. M. (2025). Pairing openet remotely sensed evapotranspiration with streamflow data to assess the effectiveness of irrigation curtailment for aquatic conservation. Journal of Hydrology, 663, 134119. https://doi.org/10.1016/j.jhydrol.2025.134119

Bales, R. C., Molotch, N. P., Painter, T. H., Dettinger, M. D., Rice, R., & Dozier, J. (2006). Mountain hydrology of the Western United States. *Water Resources Research*, *42*(8). https://doi.org/10.1029/2005wr004387

Barnett, T. P., Adam, J. C., & Lettenmaier, D. P. (2005). *Potential impacts of a warming climate on water availability in snow-dominated regions*. Nature News. https://www.nature.com/articles/nature04141

Barnhart, T. B., Molotch, N. P., Livneh, B., Harpold, A. A., Knowles, J. F., & Schneider, D. (2016). Snowmelt rate dictates streamflow. *Geophysical Research Letters*, *43*(15), 8006–8016. https://doi.org/10.1002/2016gl069690

Berghuijs, W. R., Woods, R. A., & Hrachowitz, M. (2014). A precipitation shift from snow towards rain leads to a decrease in streamflow. *Nature Climate Change*, *4*(7), 583–586. https://doi.org/10.1038/nclimate2246

Bolaños Chavarría, S., Werner, M., Salazar, J. F., & Betancur Vargas, T. (2022). Benchmarking global hydrological and land surface models against Grace in a medium-sized tropical basin. *Hydrology and Earth System Sciences*, *26*(16), 4323–4344. https://doi.org/10.5194/hess-26-4323-2022

Brooks, P. D., Gelderloos, A., Wolf, M. A., Jamison, L. R., Strong, C., Solomon, D. K., Bowen, G. J., Burian, S., Tai, X., Arens, S., Briefer, L., Kirkham, T., & Stewart, J. (2021). Groundwater-mediated memory of past climate controls water yield in snowmelt-dominated catchments. Water Resources Research, 57(10). https://doi.org/10.1029/2021wr030605

Brooks, P. D., Solomon, D. K., Kampf, S., Warix, S., Bern, C., Barnard, D., Barnard, H. R., Carling, G. T., Carroll, R. W., Chorover, J., Harpold, A., Lohse, K., Meza, F., McIntosh, J., Neilson, B., Sears, M., & Wolf, M. (2025a). Groundwater dominates snowmelt runoff and controls streamflow efficiency in the Western United States. *Communications Earth & Environment*, *6*(1). https://doi.org/10.1038/s43247-025-02303-3

Brunner, M. I., & Fischer, S. (2022). Snow-influenced floods are more strongly connected in space than purely rainfall-driven floods. *Environmental Research Letters*, *17*(10), 104038. https://doi.org/10.1088/1748-9326/ac948f

Cho, E., Vuyovich, C. M., Kumar, S. V., Wrzesien, M. L., Kim, R. S., & Jacobs, J. M. (2022). Precipitation biases and snow physics limitations drive the uncertainties in macroscale modeled snow water equivalent. *Hydrology and Earth System Sciences*, *26*(22), 5721–5735. https://doi.org/10.5194/hess-26-5721-2022

Climate assessment report | NOAA. (2013). https://psl.noaa.gov/csi/factsheets/pdf/noaa-mrb-climate-assessment-report.pdf

Clow, D. W., Nanus, L., Verdin, K. L., & Schmidt, J. (2012). Evaluation of snodas snow depth and snow water equivalent estimates for the Colorado Rocky Mountains, USA. *Hydrological Processes*, *26*(17), 2583–2591. https://doi.org/10.1002/hyp.9385

https://doi.org/10.5194/egusphere-2026-4186
Preprint. Discussion started: 24 August 2026

Daly, C., Halbleib, M., Smith, J. I., Gibson, W. P., Doggett, M. K., Taylor, G. H., Curtis, J., & Pasteris, P. P. (2008). Physiographically sensitive mapping of climatological temperature and precipitation across the conterminous United States. International Journal of Climatology, 28(15), 2031–2064. https://doi.org/10.1002/joc.1688

Denver, C., Springer, A. E., Dymond, S. F., & O'Donnell, F. C. (2025). Groundwater recharge in a fire-adapted, semi-arid forest: A Watershed Water Balance Approach. *Groundwater*, *63*(5), 736–751. https://doi.org/10.1111/gwat.70011

Dozier, J., Melack, J. M., University of California, Santa Barbara Center for Remote Sensing and Environmental Optics, & California Air Resources Board. (1989). *Snow, snowmelt, rain, runoff, and chemistry in a Sierra Nevada watershed*. The Center.

Eagleson, P. S. (1978). Climate, soil, and vegetation: 1. introduction to water balance dynamics. *Water Resources Research*, *14*(5), 705–712. https://doi.org/10.1029/wr014i005p00705

Erlingis, J. M., Rodell, M., Peters-Lidard, C. D., Li, B., Kumar, S. V., Famiglietti, J. S., Granger, S. L., Hurley, J. V., Liu, P., & Mocko, D. M. (2021). A high-resolution land data assimilation system optimized for the Western United States. *JAWRA Journal of the American Water Resources Association*, *57*(5), 692–710. https://doi.org/10.1111/1752-1688.12910

Erlingis, J., B. Li, M. Rodell, NASA/GSFC/HSL (2024): WLDAS Noah-MP-3.6 Land Surface Model L4 Daily 0.01 degree x 0.01 degree Version D1.0, Greenbelt, Maryland, USA, Goddard Earth Sciences Data and Information Services Center (GES DISC), Accessed: [March 17, 2026], doi:10.5067/ABBHPUIGJH5M

Essou, G. R. C., Arsenault, R., & Brissette, F. P. (2016). Comparison of climate datasets for lumped hydrological modeling over the continental United States. *Journal of Hydrology*, *537*, 334–345. https://doi.org/10.1016/j.jhydrol.2016.03.063

Farmer, D., Sivapalan, M., & Jothityangkoon, C. (2003). Climate, soil, and vegetation controls upon the variability of water balance in temperate and semiarid landscapes: Downward approach to water balance analysis. *Water Resources Research*, *39*(2). https://doi.org/10.1029/2001wr000328

Fassnacht, S. R., & Records, R. M. (2015). Large snowmelt versus rainfall events in the mountains. *Journal of Geophysical Research: Atmospheres*, *120*(6), 2375–2381. https://doi.org/10.1002/2014jd022753

Fassnacht, S. R., Dressler, K. A., & Bales, R. C. (2003). Snow water equivalent interpolation for the Colorado River Basin from snow telemetry (SNOTEL) data. *Water Resources Research*, *39*(8). https://doi.org/10.1029/2002wr001512

Ferguson, C. R., & Mocko, D. M. (2017). Diagnosing an artificial trend in NLDAS-2 afternoon precipitation. *Journal of Hydrometeorology*, *18*(4), 1051–1070. https://doi.org/10.1175/jhm-d-16-0251.1

Fritze, H., Stewart, I. T., & Pebesma, E. (2011). Shifts in western North American snowmelt runoff regimes for the recent warm decades. *Journal of Hydrometeorology*, *12*(5), 989–1006. https://doi.org/10.1175/2011jhm1360.1

Gao, J., Sheshukov, A. Y., Yen, H., & White, M. J. (2017). Impacts of alternative climate information on hydrologic processes with SWAT: A comparison of NCDC, prism and NEXRAD datasets. CATENA, 156, 353–364. https://doi.org/10.1016/j.catena.2017.04.010

https://doi.org/10.5194/egusphere-2026-4186
Preprint. Discussion started: 24 August 2026

Hammond, J. C., & Kampf, S. K. (2020). Subannual streamflow responses to rainfall and snowmelt inputs in snow-dominated watersheds of the Western United States. *Water Resources Research*, *56*(4). https://doi.org/10.1029/2019wr026132

He, C., Lin, T.-S., Mocko, D. M., Abolafia-Rosenzweig, R., Wegiel, J. W., & Kumar, S. V. (2025). Benchmarking and evaluating the NASA land information system (version 7.5.2) coupled with the refactored Noah-MP Land Surface Model (version 5.0). *Geoscientific Model Development*, *18*(21), 8439–8460. https://doi.org/10.5194/gmd-18-8439-2025

He, C., Valayamkunnath, P., Barlage, M., Chen, F., Gochis, D., Cabell, R., Schneider, T., Rasmussen, R., Niu, G.-Y., Yang, Z.-L., Niyogi, D., & Ek, M. (2023, March). *Noah-Multiparameterization Land Surface Model (noah-MP® LSM)*. Noah-Multiparameterization Land Surface Model (Noah-MP® LSM) | Research Applications Laboratory. https://ral.ucar.edu/model/noah-multiparameterization-land-surface-model-noah-mp-lsm

Hedrick, A. R., Marks, D., Marshall, H., McNamara, J., Havens, S., Trujillo, E., Sandusky, M., Robertson, M., Johnson, M., Bormann, K. J., & Painter, T. H. (2020). From drought to flood: A water balance analysis of the Tuolumne River basin during extreme conditions (2015 – 2017). *Hydrological Processes*. https://doi.org/10.1002/hyp.13749

Jefferson, A., Nolin, A., Lewis, S., & Tague, C. (2008). Hydrogeologic controls on streamflow sensitivity to climate variation. Hydrological Processes, 22(22), 4371–4385. https://doi.org/10.1002/hyp.7041

Jordan, Rachel. (1991). *A one-dimensional temperature model for a snow cover: Technical documentation for SNTHERM.89*. Cold Regions Research and Engineering Laboratory (U.S.).

Kapnick, S. B., & Delworth, T. L. (2013). Controls of global snow under a changed climate. *Journal of Climate*, *26*(15), 5537–5562. https://doi.org/10.1175/jcli-d-12-00528.1

Keum, J., Coulibaly, P., Razavi, T., Tapsoba, D., Gobena, A., Weber, F., & Pietroniro, A. (2018). Application of SNODAS and hydrologic models to enhance entropy-based Snow Monitoring Network Design. *Journal of Hydrology*, *561*, 688–701. https://doi.org/10.1016/j.jhydrol.2018.04.037

Kottegoda, N. T., & Elgy, J. (1977, July). Infilling missing flow data. In Modeling Hydrologic Processes, edited by: Morel-Seytoux, HJ, Salas, JD, Sanders, TG, and Smith, RE, Proc. Fort Collins 3rd Int. Hydrol. Symp., On Theoretical and Applied Hydrology, Colorado State University, Fort Collins, Colorado, USA (pp. 27-29).

Leach, J. M., Kornelsen, K. C., & Coulibaly, P. (2018). Assimilation of near-real time data products into models of an urban basin. *Journal of Hydrology*, *563*, 51–64. https://doi.org/10.1016/j.jhydrol.2018.05.064

Li, B., Rodell, M., Peters-Lidard, C., Erlingis, J., Kumar, S., & Mocko, D. (2021). Groundwater recharge estimated by land surface models: An evaluation in the conterminous United States. *Journal of Hydrometeorology*, *22*(2), 499–522. https://doi.org/10.1175/jhm-d-20-0130.1

Li, D., Wrzesien, M. L., Durand, M., Adam, J., & Lettenmaier, D. P. (2017). How much runoff originates as snow in the western United States, and how will that change in the future? *Geophysical Research Letters*, *44*(12), 6163–6172. https://doi.org/10.1002/2017gl073551

Li, J., Miao, C., Zhang, G., Fang, Y., Shangguan, W., & Niu, G. (2022). Global evaluation of the noah-mp land surface model and suggestions for selecting parameterization schemes. *Journal of Geophysical Research: Atmospheres*, *127*(5). https://doi.org/10.1029/2021jd035753

Liston, G. E., & Elder, K. (2006). A distributed snow-evolution modeling system (SnowModel). *Journal of Hydrometeorology*, *7*(6), 1259–1276. https://doi.org/10.1175/jhm548.1

Lu, H., Zheng, D., Yang, K., & Yang, F. (2020). Last-decade progress in understanding and modeling the land surface processes on the Tibetan Plateau. *Hydrology and Earth System Sciences*, *24*(12), 5745–5758. https://doi.org/10.5194/hess-24-5745-2020

Ma, N., Niu, G., Xia, Y., Cai, X., Zhang, Y., Ma, Y., & Fang, Y. (2017). A systematic evaluation of Noah-MP in simulating land-atmosphere energy, water, and carbon exchanges over the continental United States. *Journal of Geophysical Research: Atmospheres*, *122*(22). https://doi.org/10.1002/2017jd027597

Mankin, J. S., Viviroli, D., Singh, D., Hoekstra, A. Y., & Diffenbaugh, N. S. (2015). The potential for snow to supply human water demand in the present and future. Environmental Research Letters, 10(11), 114016. https://doi.org/10.1088/1748 9326/10/11/114016

Martin, D.J., Regan, R.S., Haynes, J.V., Read, A.L., Henson, W.R., Stewart, J.S., Brandt, J.T., and Niswonger, R.G. (2023, October 31). *Irrigation water use reanalysis for the 2000-20 period by huc12, month, and year for the conterminous United States (ver. 2.0, September 2024)*. USGS. https://www.usgs.gov/data/irrigation-water-use-reanalysis-2000-20-period-huc12-month-and-year-conterminous-united-states

Melton, F. S., Huntington, J., Grimm, R., Herring, J., Hall, M., Rollison, D., Erickson, T., Allen, R., Anderson, M., Fisher, J. B., Kilic, A., Senay, G. B., Volk, J., Hain, C., Johnson, L., Ruhoff, A., Blankenau, P., Bromley, M., Carrara, W., … Anderson, R. G. (2021). Openet: Filling a critical data gap in water management for the Western United States. JAWRA Journal of the American Water Resources Association, 58(6), 971–994. https://doi.org/10.1111/1752-1688.12956

Mirshafee, S., Ansari, H., Davary, K., Ziaei, A.-N., Faridhosseini, A., & Choi, Y.-S. (2024). Estimation of water balance components by Noah-MP Land Surface Model for the neyshaboor watershed, Khorasan Razavi, Iran. *Applied Water Science*, *14*(2). https://doi.org/10.1007/s13201-023-02076-0

Mocko, D. M., Kumar, S. V., Maina, F. Z., Whitney, K., Hain, C., Beck, J. M., Collins, C., Getirana, A., & Locke, K. (2024). *Development of the third phase of the North American Land Data Assimilation System (NLDAS-3)*. ADS. https://ui.adsabs.harvard.edu/abs/2024wsc..confl4113M/abstract

Montazar, A., Shields, J. W., Daccache, A., Gebremichael, M., & Putnam, D. H. (2026). Field-scale evaluation of openet for quantifying consumptive water savings under deficit irrigation in Alfalfa. Agricultural Water Management, 328, 110337. https://doi.org/10.1016/j.agwat.2026.110337

National Operational Hydrologic Remote Sensing Center (NOHRSC), 2004, Snow Data Assimilation System (SNODAS) Data Products at NSIDC, 19-JAN-2011: National Snow and Ice Data Center, Boulder, Colorado.

National Water Information System: Web Interface. USGS water data for the nation. (n.d.). https://waterdata.usgs.gov/nwis

https://doi.org/10.5194/egusphere-2026-4186
Preprint. Discussion started: 24 August 2026

Navari, M., Kumar, S., Wang, S., Geiger, J., Mocko, D. M., Arsenault, K. R., & Kemp, E. M. (2024). Enabling advanced snow physics within land surface models through an interoperable model-physics coupling framework. *Journal of Advances in Modeling Earth Systems*, *16*(4). https://doi.org/10.1029/2022ms003236

Nearing, G. S., Mocko, D. M., Peters-Lidard, C. D., Kumar, S. V., & Xia, Y. (2016). Benchmarking NLDAS-2 soil moisture and evapotranspiration to separate uncertainty contributions. *Journal of Hydrometeorology*, *17*(3), 745–759. https://doi.org/10.1175/jhm-d-15-0063.1

Niu, G.-Y., Yang, Z.-L., Mitchell, K. E., Chen, F., Ek, M. B., Barlage, M., Kumar, A., Manning, K., Niyogi, D., Rosero, E., Tewari, M., & Xia, Y. (2011). The community Noah Land Surface Model with multiparameterization options (Noah-MP): 1. model description and evaluation with local-scale measurements. *Journal of Geophysical Research*, *116*(D12). https://doi.org/10.1029/2010jd015139

NOAA National Climate Report (2020), State of the Climate: National Climate Report for Annual 2019, retrieved on March 26, 2026 from https://www.ncdc.noaa.gov/sotc/national/201913

North American Land Change Monitoring System. North American Land Change Monitoring System | Multi-Resolution Land Characteristics (MRLC) Consortium. (2020). https://www.mrlc.gov/data/north-american-land-change-monitoring-system

Peel, M. C., Finlayson, B. L., & McMahon, T. A. (2007). Updated world map of the Köppen-Geiger climate classification. *Hydrology and Earth System Sciences*, *11*(5), 1633–1644. https://doi.org/10.5194/hess-11-1633-2007

PRISM Group, Oregon State University. Accessed: [Feb 2, 2026], https://prism.oregonstate.edu

Quintana-Seguí, P., Barella-Ortiz, A., Regueiro-Sanfiz, S., & Miguez-Macho, G. (2019). The utility of land-surface model simulations to provide drought information in a water management context using global and local forcing datasets. *Water Resources Management*, *34*(7), 2135–2156. https://doi.org/10.1007/s11269-018-2160-9

Reager, J. T., Thomas, A. C., Sproles, E. A., Rodell, M., Beaudoing, H. K., Li, B., & Famiglietti, J. S. (2015). Assimilation of GRACE Terrestrial Water Storage Observations into a Land Surface Model for the Assessment of Regional Flood Potential. *Remote Sensing*, *7*(11), 14663-14679. https://doi.org/10.3390/rs71114663

Serreze, M. C., Clark, M. P., Armstrong, R. L., McGinnis, D. A., & Pulwarty, R. S. (1999). Characteristics of the Western United States snowpack from snowpack telemetry (SNOTEL) data. *Water Resources Research*, *35*(7), 2145–2160. https://doi.org/10.1029/1999wr900090

Sivapalan, M., Yaeger, M. A., Harman, C. J., Xu, X., & Troch, P. A. (2011). Functional model of water balance variability at the Catchment Scale: 1. evidence of hydrologic similarity and space-time symmetry. *Water Resources Research*, *47*(2). https://doi.org/10.1029/2010wr009568

Stern, M. A., Flint, L. E., Flint, A. L., Boynton, R. M., Stewart, J. A. E., Wright, J. W., & Thorne, J. H. (2022). Selecting the Optimal Fine-Scale Historical Climate Data for Assessing Current and Future Hydrological Conditions. Journal of Hydrometeorology, 23(3), 293–308.

https://doi.org/10.5194/egusphere-2026-4186
Preprint. Discussion started: 24 August 2026

Stewart, I. T., Cayan, D. R., & Dettinger, M. D. (2004). Changes in snowmelt runoff timing in western North America under a `business as usual' climate change scenario. *Climatic Change*, *62*(1–3), 217–232. https://doi.org/10.1023/b:clim.0000013702.22656.e8

Sthapit, E., Lakhankar, T., Hughes, M., Khanbilvardi, R., Cifelli, R., Mahoney, K., Currier, W. R., Viterbo, F., & Rafieeinasab, A. (2022). Evaluation of snow and streamflows using Noah-MP and WRF-hydro models in Aroostook River Basin, Maine. *Water*, *14*(14), 2145. https://doi.org/10.3390/w14142145

Su, L., Lettenmaier, D. P., Pan, M., & Bass, B. (2024). Improving runoff simulation in the Western United States with noah-MP and Vic Models. *Hydrology and Earth System Sciences*, *28*(13), 3079–3097. https://doi.org/10.5194/hess-28-3079-2024

Velásquez, N., Quintero, F., Koya, S. R., Roy, T., & Mantilla, R. (2023). Snow-detonated floods: Assessment of the U.S. Midwest March 2019 event. *Journal of Hydrology: Regional Studies*, *47*, 101387. https://doi.org/10.1016/j.ejrh.2023.101387

Volk, J. M., Huntington, J. L., Melton, F. S., Allen, R., Anderson, M., Fisher, J. B., Kilic, A., Ruhoff, A., Senay, G. B., Minor, B., Morton, C., Ott, T., Johnson, L., Comini de Andrade, B., Carrara, W., Doherty, C. T., Dunkerly, C., Friedrichs, M., Guzman, A., … Yang, Y. (2024). Assessing the accuracy of openet satellite-based evapotranspiration data to support water resource and land management applications. Nature Water, 2(2), 193–205. https://doi.org/10.1038/s44221-023-00181-7

Wu, W.-Y., Yang, Z.-L., & Barlage, M. (2021). The impact of Noah-MP physical parameterizations on modeling water availability during droughts in the Texas-gulf region. *Journal of Hydrometeorology*. https://doi.org/10.1175/jhm-d-20-0189.1

Xia, Y., and Coauthors, 2012: Continental-scale water and energy flux analysis and validation for the North American Land Data Assimilation System project phase 2 (NLDAS-2): 1. Intercomparison and application of model products. J. Geophys. Res., 117, D03109, doi:10.1029/2011JD016048.

Zahmatkesh, Z., Tapsoba, D., Leach, J., & Coulibaly, P. (2019). Evaluation and bias correction of SNODAS snow water equivalent (SWE) for streamflow simulation in Eastern Canadian basins. *Hydrological Sciences Journal*, *64*(13), 1541–1555. https://doi.org/10.1080/02626667.2019.1660780

Zheng, H., Fei, W., Yang, Z.-L., Wei, J., Zhao, L., Li, L., & Wang, S. (2023). An ensemble of 48 physically perturbed model estimates of the 1⁄8° terrestrial water budget over the conterminous United States, 1980–2015. *Earth System Science Data*, *15*(7), 2755–2780. https://doi.org/10.5194/essd-15-2755-2023

Zheng, X., Wang, Q., Zhou, L., Sun, Q., & Li, Q. (2018). Predictive contributions of snowmelt and rainfall to streamflow variations in the Western United States. *Advances in Meteorology*, *2018*, 1–14. https://doi.org/10.1155/2018/3765098